



**HAL**  
open science

## Operating heterogeneities within a direct borohydride fuel cell

S. Ould-Amara, J. Dillet, Sophie Didierjean, Marian Chatenet, G. Maranzana

### ► To cite this version:

S. Ould-Amara, J. Dillet, Sophie Didierjean, Marian Chatenet, G. Maranzana. Operating heterogeneities within a direct borohydride fuel cell. *Journal of Power Sources*, 2019, 439, pp.227099. 10.1016/j.jpowsour.2019.227099 . hal-02385922

**HAL Id: hal-02385922**

**<https://hal.science/hal-02385922>**

Submitted on 20 Jul 2022

**HAL** is a multi-disciplinary open access archive for the deposit and dissemination of scientific research documents, whether they are published or not. The documents may come from teaching and research institutions in France or abroad, or from public or private research centers.

L'archive ouverte pluridisciplinaire **HAL**, est destinée au dépôt et à la diffusion de documents scientifiques de niveau recherche, publiés ou non, émanant des établissements d'enseignement et de recherche français ou étrangers, des laboratoires publics ou privés.



Distributed under a Creative Commons Attribution - NonCommercial 4.0 International License

# Operating heterogeneities within a direct borohydride fuel cell

S. Ould-Amara\*, J. Dillet\*, S. Didierjean\*, M. Chatenet\*\*, G. Maranzana\*

*\*LEMETA, CNRS, Lorraine University*

*\*\* Univ. Grenoble Alpes, Univ. Savoie Mont Blanc, CNRS, Grenoble-INP, LEPMI, 38000  
Grenoble, France*

Corresponding Author:

Pr. Gaël Maranzana

LEMETA, CNRS , Lorraine University

2 Avenue de la Forêt de Haye,

54518 Vandœuvre-lès-Nancy, France

33/0 3 72 74 42 45

Gael.Maranzana@univ-lorraine.fr

## Abstract

This paper presents an analysis of the operation of a direct borohydride fuel cell fed with an alkaline solution of sodium borohydride as the fuel and pure oxygen as the oxidant. The membrane-electrode assembly is derived from proton-exchange membrane fuel cells, *i.e.* consists of a Nafion® cation-exchange membrane and carbon-supported platinum electrodes deposited on gas diffusing layers. The average performance is observed to be quite sensitive to the cell temperature. The experimental set-up makes it possible to measure the quantity of hydrogen produced by the cell, the local current density and the local potentials relative to hydrogen reference electrodes. The behavior of the cell is heterogeneous between the inlet and outlet of the reagents, due to the progressive production of hydrogen by hydrolysis down the channel direction. The direct oxidation of borohydride is effective at low current densities, but it is the oxidation of hydrogen that achieves maximum power densities. Finally, the cathode overvoltage is limiting, because the production of soda at the cathode restricts oxygen transfer (this issue can be overcome by using alkaline or bipolar membranes).

## I. Introduction

Electrochemical energy converters (notably fuel cells) are a serious alternative to thermal machines. Their energy efficiency is in practice higher and they do neither generate fine particles nor nitrogen oxides when operating at low temperatures. The most mature fuel cell technology is the proton exchange membrane fuel cell (PEMFC), which is used in particular for mobility applications [1,2]. PEMFCs are supplied with hydrogen that can be obtained from renewable energies by electrolysis of water, and therefore emit (at least potentially) only a very small amount of greenhouse gases. In addition, the production of hydrogen by electrolysis will be a way to valorize the surplus production inherent in the variable nature of electricity production from the wind or the sun. However, the hydrogen carrier is very difficult to store in gaseous form due to its very low energy density [3,4]. One solution is to store it in liquid form by producing methanol, formic acid, or even hydrocarbons or ammonia by using an additional source of carbon dioxide or nitrogen. This is the channel called "power-to-liquids". The inverse transformation is carried out either by the preliminary reforming of the liquid fuel to obtain the stored hydrogen, or by the direct oxidation of the fuel in the fuel cell. Direct oxidation is preferable for reasons of simplicity of the system [5] but, at low temperature, it is limited by the C-O bond or simply impossible to achieve with the available electrocatalysts for number of liquid fuels. There are some exceptions, though, one of which concerns sodium borohydride in alkaline media [6]. Concentrated and stable solutions can be obtained [7], leading to a gravimetric energy of 2.4 kWh/kg by considering an effective storage capacity of 7.51%<sub>w</sub>. The direct oxidation of the borohydride at pH of 14 is feasible, from the potential of -0.41 V vs RHE and ideally releases 8 electrons according to the reaction (1):



However, depending on the electrocatalyst at stake, this electrochemical reaction is in competition with the catalytic hydrolysis of the borohydride (2) and the hydrogen evolution reaction (from water reduction below 0 V vs RHE) (3, backward) followed by the oxidation of the produced hydrogen (3, forward) above 0 V vs RHE, as is the case for Pt and Au electrocatalysts [8-10].



Direct oxidation of borohydride is therefore possible, but also desirable to maximize the energy conversion efficiency of a direct borohydride fuel cell (DBFC). Research has been conducted by various teams to develop the good catalyst that allows the borohydride oxidation at low-potential without producing too much hydrogen [11,12]. Platinum seems to favour hydrolysis but good results have been obtained with palladium [10] or palladium-nickel-boron alloy on carbon nanotubes [9]. Encouraging performances as high as 420 mW/cm<sup>2</sup> have been obtained at the level of the cell [13], although the electrodes used are often derived from hydrogen fuel cells, including hydrophobic processing. A significant margin of progress is therefore to be expected. Anodes adapted to the liquid fuel without necessarily including ionomer have to be designed; they should be more open and thicker, made of hydrophilic materials, so as to ease mass-transfer phenomena, as anticipated by Cheng and Scott [14,15] and Freitas et al. [16]. It is also desirable to determine the mass and charge transfer mechanisms so that optimization can be performed based on modelling results.

The work proposed here is positioned downstream from studies on materials. The aim is to evaluate the performance of a direct borohydride fuel cell with a local resolution between fuel inlet and outlet. The instrumented cell used makes it possible to locally measure the current density and the potential of the two electrodes with respect to reference electrodes located on the membrane along the active surface. With this setup, the operating heterogeneities that may be associated with the increase of hydrogen flow and decrease of  $\text{BH}_4^-$  concentration down the channel direction are evaluated. The start / stop phases are also characterized and highlight the potential sustainability issues of the DBFC, as for regular  $\text{H}_2$ -fed PEMFCs [17-20]. These observations at the level of the cell may help to guide the development of new electrodes. A first part is devoted to the description of the experimental device and a second to the presentation of the observations and analysis of the results.

## II. Experimental setup

The experimental test bench developed for this study is shown in Figure 1.

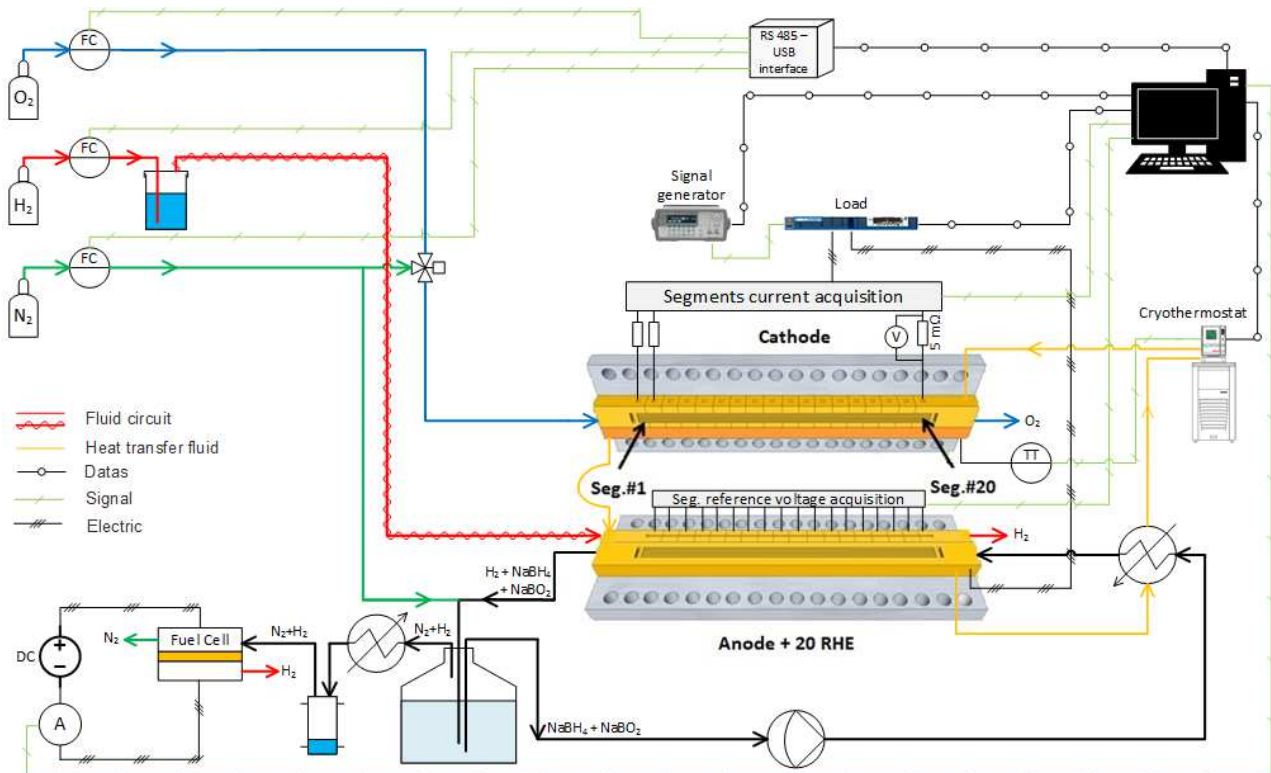


**Fig.1:** test bench used for segmented DBFC studies. The system is composed of a segmented-anode DBFC (20 segments, 1cm×1.5cm each) fed by O<sub>2</sub> at the cathode and a NaOH + NaBH<sub>4</sub> anolyte at the anode. 20 hydrogen reference electrodes enable to measure the individual potential of the anode and cathode for all the segments; they are fed with hydrogen. Downstream the DBFC, the anolyte is recycled, and any H<sub>2</sub> produced in the cell is separated from the liquid phase and diluted by nitrogen, and then quantified in a dedicated PEMFC operating in H<sub>2</sub>-pump mode.

The segmented cell constitutes LEMTA's own know-how. Our first linear instrumented cell was developed in 2007 [21]. Then, it was improved many times in order to get better performances that are now representative of a non-segmented cell. The membrane electrode assemblies (MEAs) considered here are made of a cation-exchange membrane (CEM, Nafion® NR212), just positioned as received (without initial “cleaning” of exchange into the Na<sup>+</sup> form) between an anode and a cathode gas diffusion electrodes (GDE) without any hot pressing. The catalyst is made of regular 40% Pt/C (0.5 mgPt/cm<sup>2</sup> loading), and the active layers embed hydrophobic tetrafluoroethylene (PTFE) as a binder. As the alkaline anolyte solution impregnates the electrode and comes into contact with the membrane, sodium ion Na<sup>+</sup> can be transferred without any Nafion® ionomer in the electrode. This catalyst is coated on a gas-diffusion layer (GDL) possibly comprising a microporous layer (MPL). Different GDEs have been tested as anode and cathode by varying the PTFE loading in the electrode and in the GDL. Actually, the borohydride solution cannot cross a MPL. Only anodes without MPL can produce power and the best performances have been reached with highly hydrophobic cathode (40% PTFE loading with MPL) and less hydrophobic anode (10% PTFE loading without MPL). This is explained by the fact that (i) it is necessary to evacuate the soda formed at the cathode to allow the transport of oxygen and (ii) the solution has to be able to wet the anode catalyst layer.

PTFE gaskets were used to adjust the thickness of the electrodes to get 20% of compression of the initial thickness. Twenty reference electrodes spaced 15mm apart are positioned on the membrane along the active area (Figure 2). They are fed by humidified hydrogen thanks to a segmented channel placed on the side of the anodic channels. These twenty GDE discs are placed on the part of the membrane which is not submitted to the

alkaline solution and therefore remains in  $H^+$  form. These local reference electrodes can thus be considered as RHE electrodes (pH of 14).

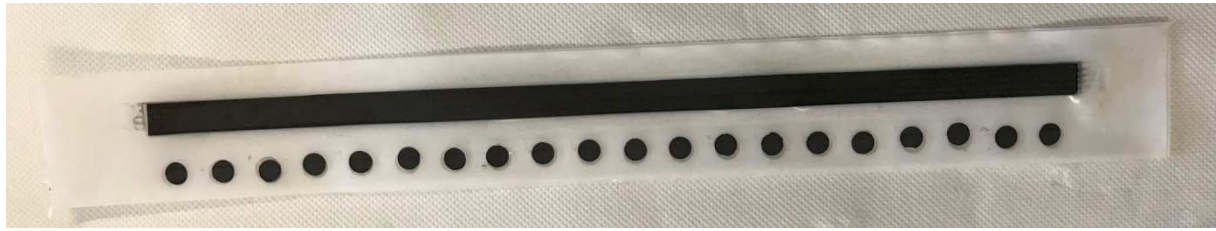


**Fig.2:** 30 cm x 1 cm MEA with 20 reference electrodes (regular GDE) along the active area

The anolyte fuel was composed of 0.5 mol/L  $NaBH_4$  (Sigma aldrich, 98% purity) in 4 mol/L  $NaOH$  (VMR Analar<sup>®</sup> Normapur<sup>®</sup>) dissolved in ultrapure water (18 m $\Omega$  cm). Pure oxygen (Messer, 99.999%) was used as oxidant. The borohydride solution was injected into the fuel cell by means of a pump (mzr-4665HNP) which regulates the flow of the solution. Temperature regulation was achieved thanks to a circulating bath driven by a Pt100 probe inserted in the anodic plate. Before entering the cell, the thermo-regulated water passed through a heat exchanger, the function of which was to preheat the borohydride solution to the desired temperature. Without this heat exchanger, the performances were found to be very sensitive to the fuel flow rate, due to a progressive heating of the solution into the cell from the inlet to the outlet. As it will be presented in the next section, the performances of the cell are very sensitive to temperature. The measurement of the total amount of hydrogen released is performed using a phase separator and a  $H_2/H_2$  fuel cell. A nitrogen flow rate is added to the borohydride- $H_2$  mixture recovered at the cell outlet in order to increase the flow rate of gas and decrease the time response of the  $H_2$  flow rate measurement. The liquid returns to the anolyte reservoir and the gas is sent to the  $H_2/H_2$  fuel cell operating at  $U_{cell} = 0.6$  V. The current consumed by the hydrogen pump makes it possible to evaluate the flow of hydrogen escaping the DBFC anode.

### III. Results and discussion

#### III.1. Start-up

The cell was first purged with distilled water to check for leaks. Then the borohydride solution was injected at a flow rate of 1 L/h. As shown in figure 3.b, before the borohydride injection the anode and cathode potentials with respect to the reference were equal to about  $E_{+ \text{ or } -} = 1 \text{ V vs SHE}$ , which corresponds to the potential of an oxygen electrode in an acidic medium. Indeed the Nafion® membrane being used as received was therefore initially in its protonic form. Getting in the cell, the borohydride anolyte solution produces an overshoot of voltage up to 1.8 V, as shown in Figure 3.a. This overshoot is explained by the superposition of two phenomena:

- At the beginning of the filling process, the cell comprises a cathode in acidic medium ( $E_{+} \approx + 1 \text{ V vs SHE}$ ) and an anode in basic medium with presence of borohydride ( $E_{-} \approx -1.2 \text{ V vs SHE}$ ), what means potentially a 2.2 V cell voltage. During this transient phase, the protons in the membrane are gradually replaced by sodium ions from the anolyte, and the potential of the cathode gradually decreases to + 0.2 V vs RHE, which corresponds roughly to the potential of an oxygen electrode in alkaline medium (at that stage, the active area of the CEM is no longer acidic – all the  $\text{H}^{+}$  have been replaced by  $\text{Na}^{+}$ ). At the same time, the potential of the anode decreases from  $E_{-} = 1 \text{ V vs RHE}$  (initially, the CEM is still in  $\text{H}^{+}$  form and the anode still under oxygen) to  $E_{-} = -0.9 \text{ V vs. RHE}$  (Figure 3b), *i.e.* a potential between that of hydrogen and borohydride at pH of 14. This transient lasts 10 s. Note that after a few minutes, due to the fuel crossover, these potentials stabilize to about  $E_{-} = -1.12 \text{ V vs RHE}$  for the anode and  $E_{+} = -0.1 \text{ V vs RHE}$  for the cathode depending on the temperature, as will be discussed hereafter.

- The injection of the borohydride solution is not instantaneous. A concentration front is transported from the inlet (entrance) to the outlet (exit). During this filling time of the anode compartment, a potential heterogeneity appears between the inlet and the outlet. In the same way as when starting a hydrogen fuel cell, this results in an overshoot of cell voltage (Figure 3a), the duration of which is longer than for “equivalents” at PEMFC startups. Note that the local potential of the cathode in front of the anode outlet reached  $E_+ = 1.6 \text{ V vs. RHE}$  for a PEMFC, which is an issue for the cathode catalyst durability [17-20]. In this first startup, the local potential of the cathode varies in a complex manner (Figure 3c): at the fuel inlet, the potential firstly decreases towards  $0.1 \text{ V vs RHE}$  (at minimum), while at the outlet, it firstly increases to  $1.5 \text{ V vs RHE}$  (at maximum), the minimum in the fuel inlet region and maximum at fuel outlet region being concomitant. Then, from these extrema and for the segments towards the middle of the cell, the local cathode potentials evolve towards ca.  $0.8 \text{ V vs RHE}$  after  $t = 10 \text{ s}$  (at that stage the CEM is still in  $\text{H}^+$  form at the cathode interface); at the end of this transient ( $t > 10 \text{ s}$ ), then all segments reach similar local potential values, and progressively reach a “stabilized” potential of ca.  $0.2 \text{ V vs RHE}$  after ca.  $t = 50 \text{ s}$  (at that stage the CEM is in  $\text{Na}^+$  form at the cathode interface, and of course at the anode interface as well).

Very surprisingly, in the present DBFC configuration, no internal current could be measured during this first start up from a CEM in acidic ( $\text{H}^+$ ) form. The protons initially in the membrane can either participate in the reduction of oxygen by leaving the membrane on the cathode side, or be neutralized by the  $\text{OH}^-$  ions by leaving the membrane on the anode side after replacement with sodium ions. This last hypothesis, which does not lead to the production of current, seems to be verified.

Things are different for the second startup, when then CEM was already completely exchanged in  $\text{Na}^+$  form (alkaline). Figure 4 shows the internal currents measured during such a startup, with a membrane initially in sodium form and an initial high pH at the cathode. The internal currents and potentials are substantially identical to those observed for a startup with a hydrogen fuel cell. The amplitude of the overshoot of the cell voltage does not exceed 1.2 V and negative currents appear in the passive part not yet fed by the fuel. These locally-reversed currents are likely to lead to degradation of the DBFC electrode materials, which could be studied in a forthcoming contribution.

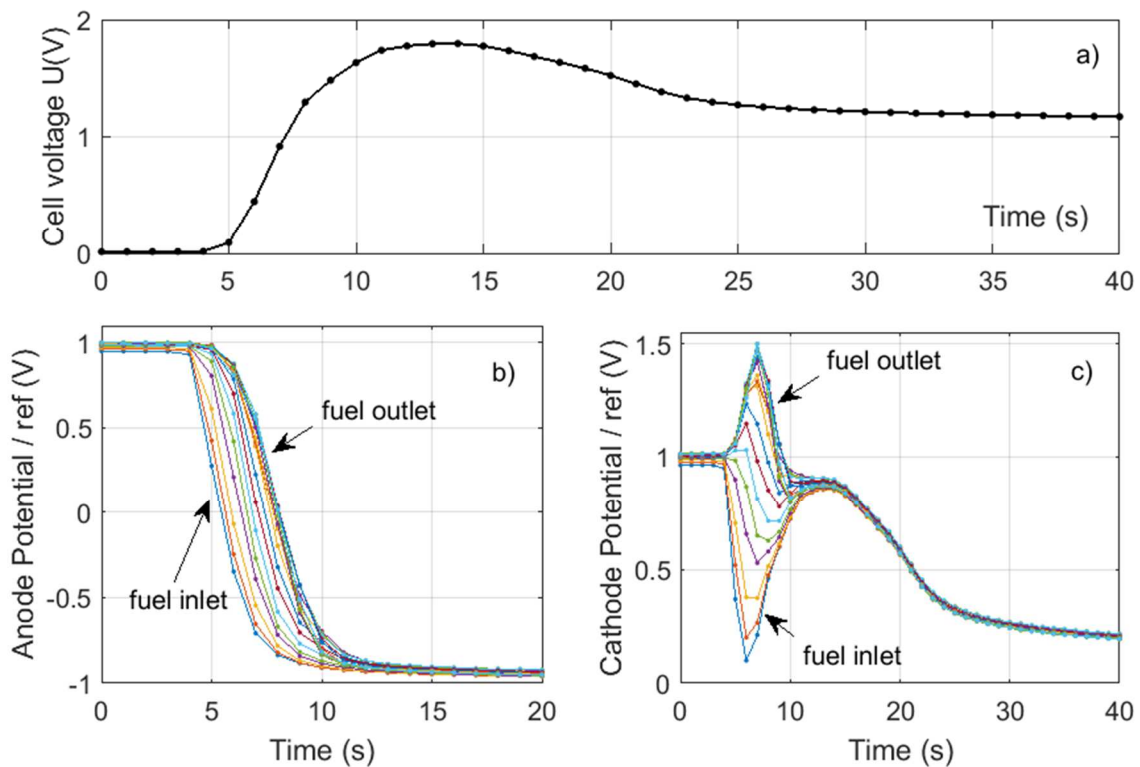


**Fig.3.** a) Cell voltage as a function of time for the first start-up with a membrane initially in its acidic form, b) Potential of the anodes with respect to the distributed reference electrodes, c) Potential of the cathodes, all results are obtained at 30°C.

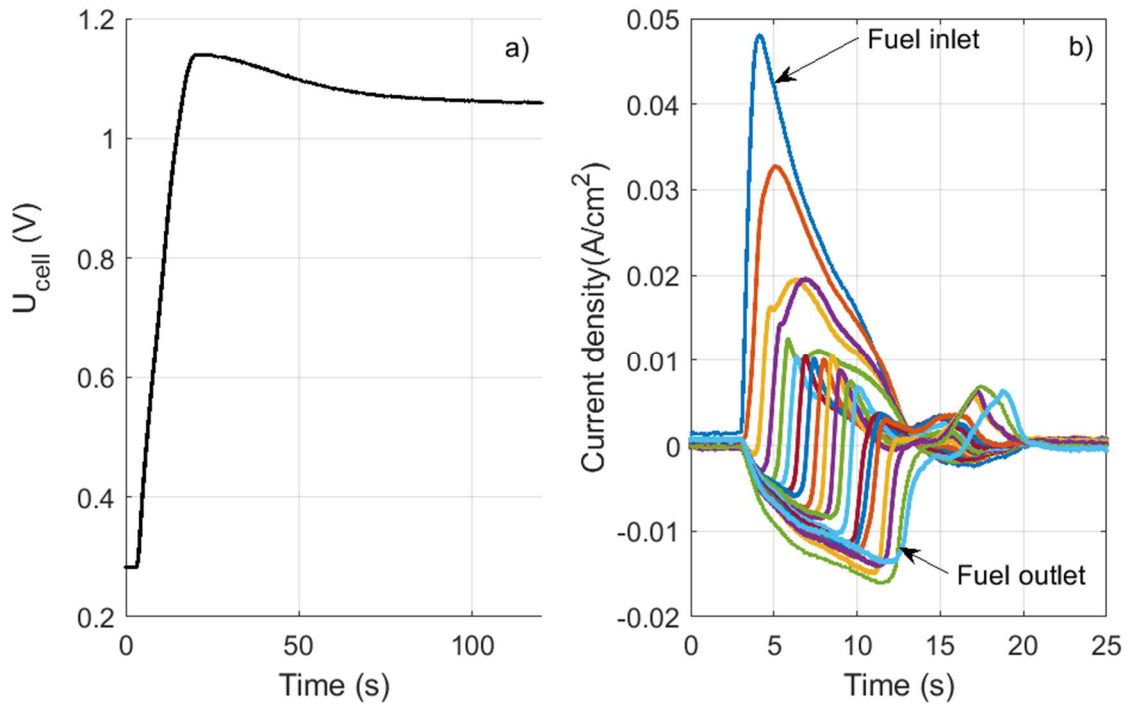


**Fig.4.** a) Cell voltage during the second start-up with a membrane in its sodium form as a function of time, b) internal current as a function of time, all results are obtained at 30°C.

### III.2. Operating performances and local heterogeneities

Cell performances were measured for four different temperatures of  $T = 30, 40, 50$  and  $60^\circ\text{C}$ . Figure 5 shows the average performances (polarization plots and anode/cathode potentials in Figure 5a, power density in Figure 5b) for an electrode membrane assembly consisting of a GDE ( $0.5 \text{ mg/cm}^2 \text{ Pt/C} - 10\% \text{ PTFE}$  – without MPL) at the anode and a GDE ( $0.5 \text{ mg/cm}^2 \text{ Pt/C} - 40\% \text{ PTFE}$  – with MPL) at the cathode. Note the high sensitivity of the results with respect to temperature. An increase in temperature has complex and antagonistic effects; it reduces the resistance of the membrane to the transfer of sodium ions but on the contrary may lead to increased crossover of the anolyte fuel to the cathode; it improves the kinetics of the various competing reactions at stake (oxidation of borohydride and hydrogen, hydrolysis of borohydride to hydrogen at the anode; reduction of oxygen at the cathode). In

Figure 5a it is shown that the potential of the cathode depends rather little on the temperature, unlike the potential of the anode. It is probable that the cathode performances are limited by the solubility of oxygen in the sodium hydroxide that wets the cathode, and that the limitation of the anode is of kinetic order. The maximum power density achieved here is  $120 \text{ mW/cm}^2$  (Figure 5b). It is possible to improve this performance by further increasing the temperature but the corrosive nature of sodium hydroxide solution at temperatures above  $T = 60^\circ\text{C}$  is an issue. Figure 5c shows that the quantity of hydrogen produced is more important as the temperature is raised. It also shows that the evolution of hydrogen is a decreasing function of the current density. The hydrogen production stops for the current density corresponding substantially to the maximum power; this means that the oxidation of hydrogen (HOR) produced by (heterogeneous) hydrolysis of  $\text{NaBH}_4$  is likely to play an important role in obtaining a good power density, at least with the platinum catalyst used in the present anode. However, it is possible to increase the current density beyond the density which cancels the hydrogen evolution, which would prove that the oxidation of hydrogen is not the only reaction at the origin of the anodic current, and that "direct" oxidation of  $\text{BH}_4^-$  (BOR) is also possible at Pt anodes, even if the kinetics of the BOR is less favorable than that of HOR on platinum [8-10]. Figure 5a shows an increasing anode potential as a function of the current density and a singular evolution of the cathodic potential: it is first decreasing, *i.e.* the activation overvoltage increases with the current density. Then it stabilizes and even increases slightly for high current densities. This effect may be explained by the suppression of the hydrogen crossover, which had the effect of decreasing the cathodic potential. Since all the hydrogen produced is oxidized at high current densities, crossover can no longer occur.

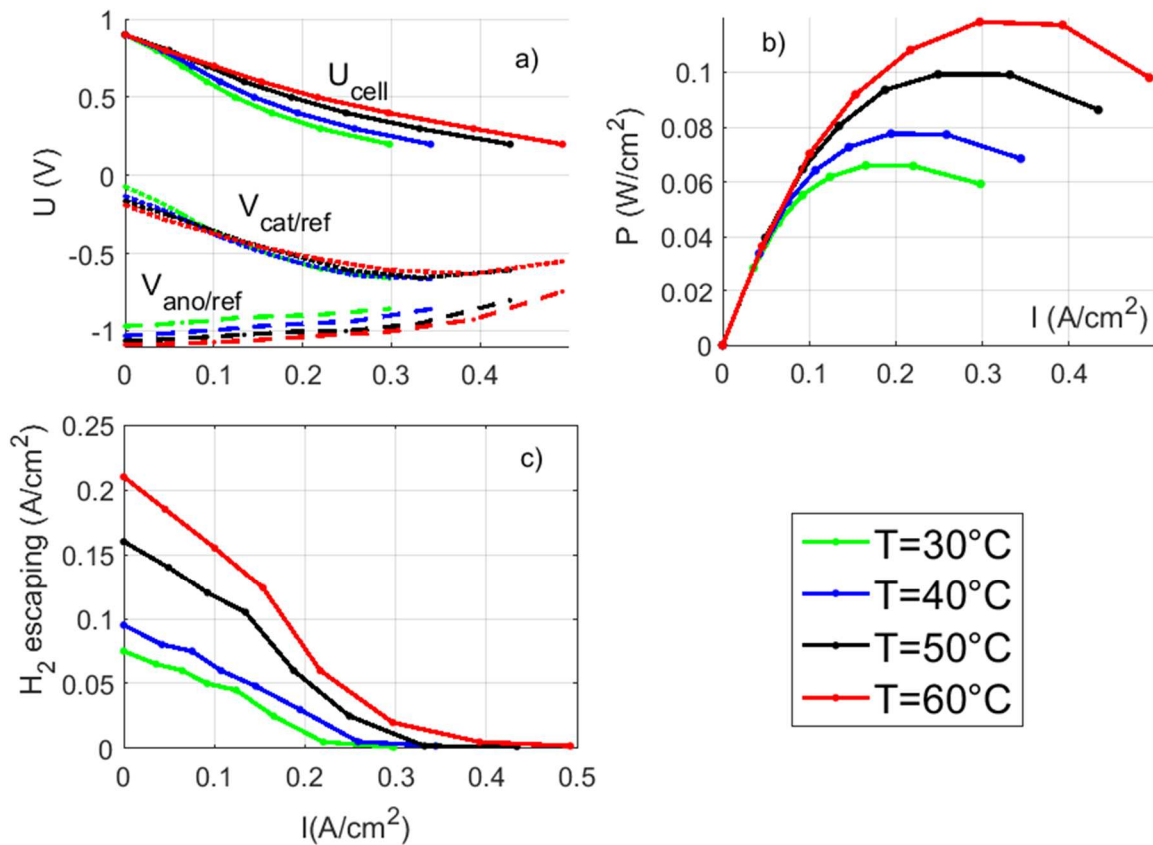


**Fig.5.** a) polarization curve and average anodic and cathodic potentials with respect to  $\text{H}_2$  reference electrodes. b) Power density. c) Detection of hydrogen escaping the anode outlet (an  $\text{H}_2$  escaping current of  $0.2 \text{ A}/\text{cm}^2$  means a total hydrogen flow rate of  $5\text{NL}/\text{h}$  at the cell outlet)

### **Heterogeneities of operation between the inlet and outlet.**

Figure 6a shows the current densities as a function of the position for several average currents. On the one hand, it is observed that the current density does not evolve in large proportions from the inlet to the outlet (25% variation). It is slightly decreasing between fuel inlet and outlet for low current densities and increasing for high current densities. On the other hand, the respective potentials of anode and cathode are quite heterogeneous (Figure 6b). The anode potential at the inlet “where there is little hydrogen” is below that at the

outlet for low current densities: it is  $-1.13$  V vs RHE, which is below the equilibrium potential of hydrogen and demonstrates that “direct” oxidation of  $\text{NaBH}_4$  proceeds in this region and in these experimental conditions. In this case of low current densities, it is therefore more advantageous to directly oxidize the borohydride, the associated activation overvoltage being not yet too penalizing. Then, when the average current density increases, the anodic potential of the inlet increases rather strongly compared to the outlet, because the oxidation of the hydrogen present in large quantity at the outlet is much easier on platinum than the direct borohydride oxidation. This confirms that this is hydrogen oxidation that makes it possible to obtain a good power density, at least with the platinum catalyst used herein. In addition, the direct oxidation of borohydride is interesting at low current densities, to valorize the associated lower oxidation-reduction potential (and this must be strongly depending on the anode catalyst used [22], although it is beyond the scope of the present paper to study so). Finally, it is observed that the anodic potential increases a lot for the cell voltage of  $0.3 > U_{\text{cell}} > 0.2$  V, which corresponds to the end of hydrogen production (see figure 5c). For these high current densities, all the hydrogen produced is oxidized in the cell. Here, hydrogen is responsible for the anode potential of  $-1.08$  V vs RHE which is rather constant as a function of the current density. As long as hydrogen is present, it is thus the cathode which is limiting.

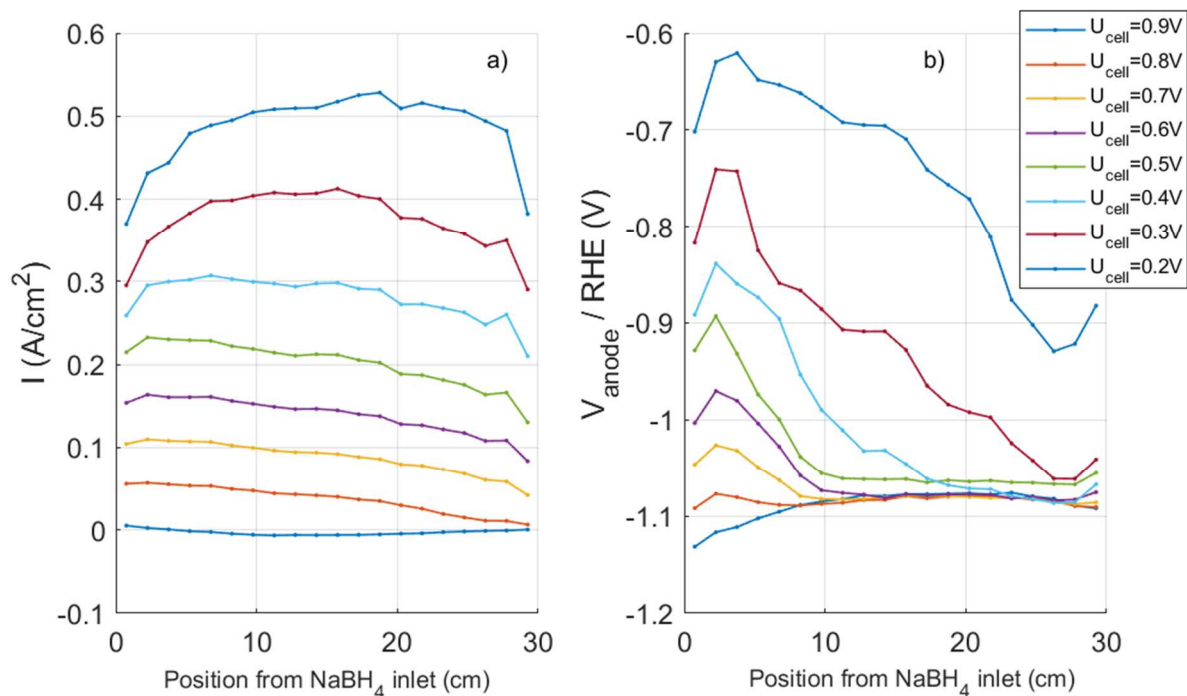


**Fig.6:** performances of the segmented DBFC in terms of (a) local current density, (b) local anode potential with respect to the **RHE**,  $T = 60^\circ\text{C}$

### III.3. Flow rate sensitivity

The influence of a variation of the borohydride solution flow rate was evaluated and is shown in Figure 7. There is an increase in performance up to the flow rate corresponding to a stoichiometry of about 10; then, the performances stabilize and even slightly decrease, which can be explained by an imperfect thermalization of the solution at high flow rate. The flow of hydrogen produced evolves at the same pace as the cell voltage but stabilizes at a slightly higher rate. This limit reached by the hydrogen flow rate means that the hydrolysis of the borohydride is limited by the transport in the through-plane direction. This electrode manufactured similarly to a hydrogen fuel cell electrode is confined to the direct vicinity of the membrane and not very accessible to the solution. Reagents must diffuse from channels

to the electrode through the GDL. Even if this mass-transfer is favored by greater pressure losses, which create a Darcy flow in the GDL, it remains limited.

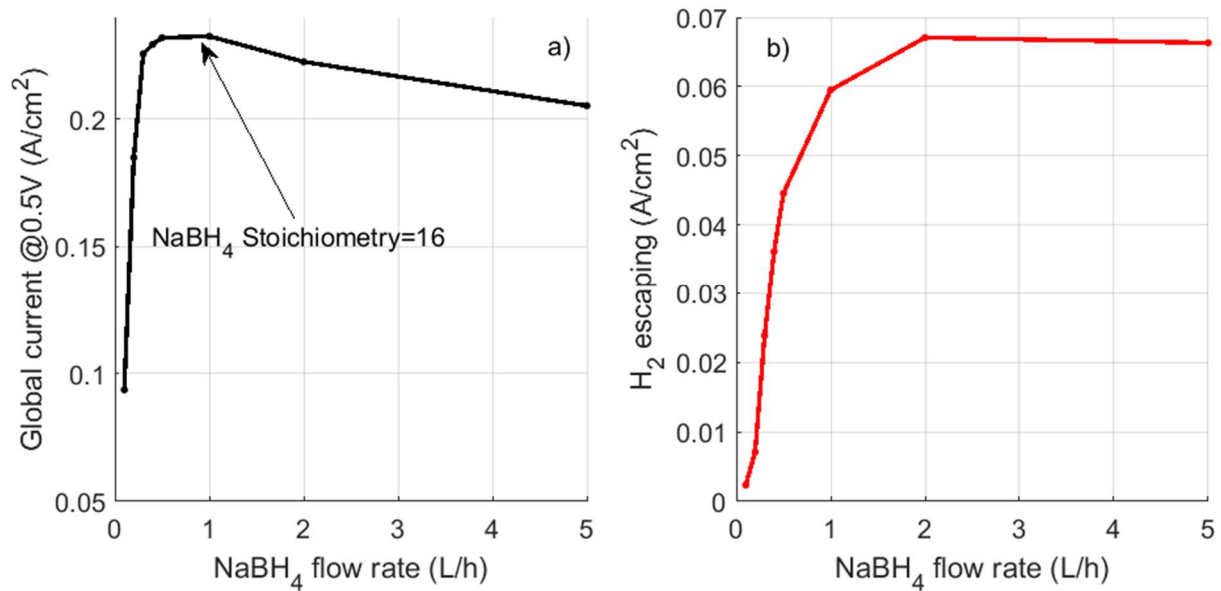


**Fig.7:** influence of the fuel flow rate sensitivity on (a) the overall current produced by the DBFC at  $U_{cell} = 0.5$  V (and (b) the H<sub>2</sub> escape,  $T = 60^{\circ}\text{C}$ .

### III.4. Purging the cathode with distilled water

Figure 5a showed that the cathode overvoltage is far from negligible, although pure oxygen is used; the cathode employs highly-efficient Pt/C based oxygen reduction reaction (ORR) catalyst and has a very hydrophobic character (hence should not be completely drown by anolyte). This overvoltage can firstly be explained by the very low solubility and diffusivity of oxygen in the sodium hydroxide produced at the cathode (by combination of the OH<sup>-</sup> products of the oxygen reduction reaction, and of the Na<sup>+</sup> ions that migrate in the CEM under current flow) [23,24]; the concentration of NaOH formed at the cathode might indeed be large (the cathode is hydrophobic), severely impacting the mass-transfer of oxygen from the gas compartment to the active sites (that are wetted by the electrolyte). Secondly, fuel

crossover is also probably, favoring mixed reactions (needless to say that Pt is active for the BOR) and subsequent catalyst poisoning with BOR intermediates and products [25]. Although the cathode is very hydrophobic (this is positive to avoid drowning, but detrimental because it cannot “dilute” the NaOH formed at the cathode when a CEM is used), an effect of purging with distilled water could be observed. Figure 8 shows the current response for a cell voltage maintained at  $U_{\text{cell}} = 0.5$  V following brief purging (3 mL injected) with liquid water. There is a very positive effect on the current produced, and this effect dissipates in a few tens of minutes. It is likely that the liquid water “pulse” enables to expel NaOH (and possibly BOR) products, thereby transiently improving the cathode performances. This further confirms that the cathode is non-negligibly limiting the present DBFC performances, and that there is room for optimization of the cathode and whole cell, as exemplified hereafter. (i) Selective catalysts insensitive to borohydride permeation would be less hindered by the anolyte crossover [26-29]; with such catalysts, (ii) using an alkaline membrane or no membrane (but instead a porous separator) could be viable [29]. (iii) Another solution envisaged by [30] is to use a bipolar membrane in order to solve both borohydride permeation and soda production, which seems mandatory to obtain high stability of the DBFC performances.

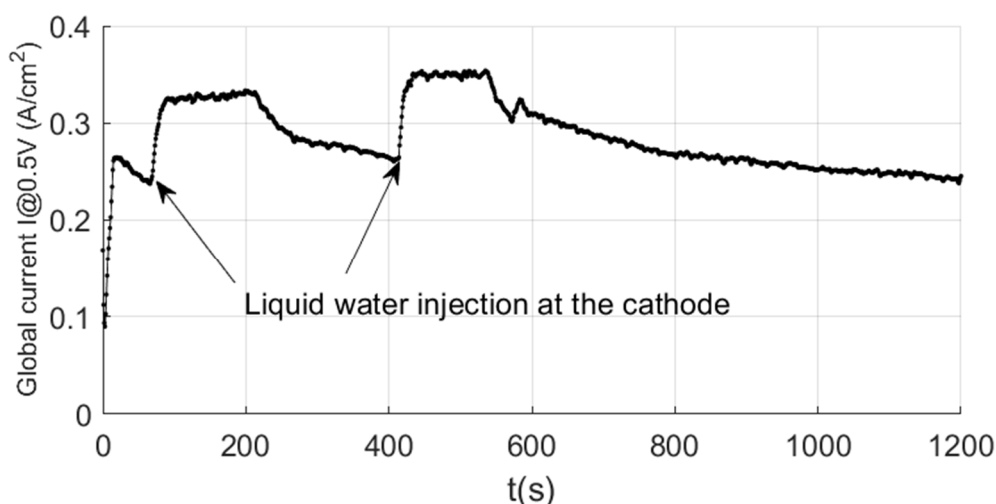


**Fig.8:** effect of liquid water injection at the cathode during operation of the DBFC at  $U_{cell} = 0.5 \text{ V}$ .  $T = 60^\circ\text{C}$

#### IV. Conclusion

This paper reports some observations of a DBFC with a spatial resolution between the inlet and the outlet of the reagents. On the regular PEM fuel cell platinum electrodes considered here, the direct oxidation of borohydride is the primary reaction at stake for low current densities. It leads to a larger cell voltage than the oxidation of hydrogen, because the BOR initiates at lower potential than the HOR. For higher current densities, the oxidation of hydrogen is best able to provide power, because the activation overvoltage is lower (the BOR kinetics is slower than the HOR kinetics). The evolution of hydrogen from the Pt-based anode is not negligible, and proceeds both from the hydrogen evolution reaction (cathodic reduction of water) at or below 0 V vs RHE and from the (heterogeneous) hydrolysis of  $\text{BH}_4^-$ ; it generates hydrogen escape (in other words,  $\text{H}_2$  can exit the cell if it is not completely valorized), but this escape decreases as a function of the current density. Indeed, Pt enables the oxidation of the produced  $\text{H}_2$  in the HOR, provided the potential is above 0 V vs RHE. It is

possible to operate without release of hydrogen, if the current density is sufficient (which means the anode potential is sufficiently above 0 V vs RHE). Otherwise, at low current density, it seems necessary to consider a solution to efficiently valorize the hydrogen produced. In the present system, the cathode is responsible for a significant part of the irreversibilities, because the Pt catalyst is not selective for the ORR (and instead is also active for the BOR), and because the production of sodium hydroxide penalizes the transport of oxygen to the catalytic sites. One way to cope with these issues would be to use an anionic membrane and a selective catalyst that is insensitive to borohydride permeation or a bipolar membrane.

## V. Acknowledgement

The authors wish to thank the ANR for the funding received under the Mobidic project (ANR-16-CE05-0009).

## References

1. P. Corbo, F. Migliardini, O. Veneri, *Hydrogen Fuel Cells for Road Vehicles*, Springer, 2011
2. B. Zohuri, *Hydrogen-Powered Fuel Cell and Hybrid Automobiles of the Near Future*, Springer, 2019.
3. G. Sdanghi, G. Maranzana, A. Celzard, V. Fierro, *Renewable and Sustainable Energy Reviews* 102, 150–170, 2019.
4. A. Godula-Jopek, W. Jehle, J. Wellnitz, *Hydrogen Storage Technologies: New Materials, Transport, and Infrastructure*, Wiley, 2012.
5. J. H. Wee, *Journal of Power Sources*, 155, 329-339, 2006.

6. J. Ma, N. Choudhury, Y. Sahai , *Renewable and Sustainable Energy Reviews*, 14, 183–199, 2010.
7. P. Y. Olu, N. Job, M. Chatenet, *Journal of Power Sources*, 327, 235-257, 2016.
8. P.-Y. Olu, A. Bonnefont, M. Rouhet, S. Bozdech, N. Job, M. Chatenet, E. Savinova, *Electrochimica Acta*, 179, 637-646, 2015.
9. P.-Y. Olu, A. Bonnefont, G. Braesch, V. Martin, E.R. Savinova, M. Chatenet, *Journal of Power Sources*, 375, 300-309, 2018.
10. G. Braesch, A. Bonnefont, V. Martin, E.R. Savinova, M. Chatenet, *Electrochimica Acta*, 273 483-494, 2018.
11. K. Mochalov, V. Khain, G. Gill'manshin, *Dokl. Akad. Nauk SSSR.*, 162, 613-616, 1965.
12. Y. Zhou, S.Li, Y. Chen, Y. Liu, *Journal of Power Sources*, 351, 79-85, 2017.
13. P.Y. Olu, F. Deschamps, G. Caldarella, M. Chatenet, N. Job, *Journal of Power Sources*, 297, 2015.
14. H. Cheng, K. Scott, *Journal of Applied Electrochemistry*, 36, 1361-1366, 2006.
15. H. Cheng, K. Scott, *Journal of Power Sources*, 160, 407-412, 2006.
16. K.S. Freitas, B.M. Concha, E.A. Ticianelli, M. Chatenet, *Catal. Today*, 170, 110-119, 2011.
17. A. Lamibrac, G. Maranzana, O. Lottin, J. Dillet, J. Mainka, S. Didierjean, A. Thomas, C. Moyne, *Journal of Power Sources*, 196, 9451-9458, 2011.
18. G. Maranzana, A. Lamibrac, J. Dillet, S. Abbou, S. Didierjean, O. Lottin, *Journal of The Electrochemical Society*, 162 (7), F694-F706, 2015.
19. J. Dillet, D. Spornjack, A. Lamibrac, G. Maranzana, R. Mukundan, J. Fairweather, S. Didierjean, R. Borup, O. Lottin, *Journal of Power Sources*, Vol 250, 68-79, 2014.
20. J. Durst, A. Lamibrac, F. Charlot, J. Dillet, L. Castanheira, G. Maranzana, L. Dubau, F. Maillard, M. Chatenet, O. Lottin, *Applied Catalysis B: Environmental*, 138–139, 17, 2013.

21. G. Maranzana, O. Lottin, T. Colinart, S. Chupin, S. Didierjean, *Journal of Power Sources*, 180, 748-754, 2008
22. P.-Y. Olu, N. Job, M. Chatenet, *Journal of Power Sources*, 327, 235-257, 2016.
23. M. Chatenet, M. Aurousseau, R. Durand, *Industrial & Engineering Chemistry Research*, 39, 3083-3089, 2000.
24. M. Chatenet, M. Aurousseau, R. Durand, *Electrochimica Acta*, 45, 2823-2827, 2000.
25. R. Battino, T. R. Rettich, T. Tominaga, *Journal of Physical Chemistry*, 12, 163-178, 1983.
26. Y. G. Wang, Y. Y. Xia, *Electrochemistry Communications*, 8, 1775-1778, 2006.
27. R. X. Feng, H. Dong, Y. D. Wang, X. P. Ai, Y. L. Cao, H. X. Yang, *Electrochemistry Communications*, 7, 449-452, 2005.
28. S. Li, C. Shu, Y. Chen, L. Wang, *Ionics*, 2017
29. S. Guo, J. Sun, Z. Zhang, W. Ding, *Journal of Materials Chemistry A*, 5(30), 2017.
30. Z. Wang, J. Parrondo, J. Parrondo, C. He, V. Ramani, *Nature Energy*, 2019